Ruggeri, Z. M., & Zimmerman, T. S. (1987) *Blood 70*, 895–904.
Ruggeri, Z. M., De Marco, L., Gatti, L., Bader, R., & Montgomery, R. R. (1983) *J. Clin. Invest. 72*, 1–12.
Stel, H. V., Sakariassen, K. S., de Groot, P. G., van Mourik, J. A., & Sixma, J. J. (1985) *Blood 65*, 85–90.
Studier, F. W., & Moffatt, B. A. (1986) *J. Mol. Biol. 189*, 113–130.
Titani, K., Kumar, S., Takio, K., Ericsson, L. H., Wade, R. D., Ashida, K., Walsh, K. A., Chopek, M. W., Sadler, J. E., & Fujikawa, K. (1986) *Biochemistry 25*, 3171–3184.
Trapani-Lombardo, V. T., Hodson, E., Roberts, J. R., Kunicki, T. J., Zimmerman, T. S., & Ruggeri, Z. M. (1985) *J. Clin. Invest. 76*, 1950–1958.
Vicente, V., Kostel, P. J., & Ruggeri, Z. M. (1988) *J. Biol. Chem. 263*, 18473–18479.
Vicente, V., Houghten, R. A., & Ruggeri, Z. M. (1990) *J. Biol. Chem. 265*, 274–280.
Walsh, P. N., Mills, D. C. B., & White, J. G. (1977) *Br. J. Haematol. 36*, 281–298.
Weiss, H. J., Turitto, V. T., & Baumgartner, H. R. (1978) *J. Lab. Clin. Med. 92*, 750–764.
Weiss, H. J., Turitto, V. T., & Baumgartner, H. R. (1986) *Blood 67*, 322–330.
Weiss, H. J., Hawiger, J., Ruggeri, Z. M., Turitto, V. T., Thiagarajan, P., & Hoffman, T. (1989) *J. Clin. Invest. 83*, 288–297.

Ion-Binding Properties of Calbindin D_{9k}: A Monte Carlo Simulation Study

Bo Svensson,* Bo Jönsson, Clifford E. Woodward, and Sara Linse
Physical Chemistry 2, Chemical Centre, University of Lund, P. O. Box 124, S-22100 Lund, Sweden
Received June 27, 1990; Revised Manuscript Received December 6, 1990

ABSTRACT: Monte Carlo simulations are used to calculate the binding constant of two Ca^{2+} ions to the protein bovine calbindin D_{9k}. The change in binding constant with respect to mutation of charged amino acids, presence of various electrolytes, protein concentration, solution pH, and competitive binding of monovalent ions is investigated. Each of these factors may have a large influence on the binding constant. The simulations are performed in a dielectric continuum model, the so-called primitive model of electrolyte theory, with a fixed protein structure and a uniform dielectric permittivity. The calculated binding constants are in excellent agreement with experimental data and describe changes in the binding constant over six orders of magnitude.

During the last five years or so breakthroughs in genetic engineering techniques have made possible the production of synthetic biomolecules. In particular, specifically designed proteins are now able to be manufactured in large quantities, which will have a large impact on the field of pharmacology. A need to understand changes in the function and efficacy of proteins, due to specific mutations and changes in ambient conditions (e.g., electrolyte concentration), has stimulated interest in theoretical models, which may hopefully provide some predictive power. Indeed, in the near future, one can expect that theory will become an increasingly important contributor to the advancement of the predominantly experimental field of molecular biology.

The theoretical approach to these many-atomic systems is based on statistical mechanics. However, while approximate statistical mechanical theories easily deal with systems of say spherical or cylindrical symmetry, awkward numerical procedures are generally needed to solve for more complex geometries, such as that of a protein molecule. It is easy to appreciate the possibilities offered by simulation techniques such as Monte Carlo (MC) and molecular dynamics. Both methods have already proven their utility for simple liquids (Hansen & McDonald, 1976), and their ease of applicability is not greatly affected by the symmetry of the system under study. To date the most detailed calculations utilizing these methods have included an all-atom description of the protein together with a number of surrounding solvent and solute molecules. However, simulations of these "ab initio" models (Ahlström et al., 1987) suffer from the enormous computer time needed, not to mention the problem of choosing realistic atomic interactions.

When an attempt is made to calculate equilibrium properties of proteins in solution, the formidable computational problems, alluded to above, force one to turn to simpler models. For example, when focussing on electrostatic interactions, it is possible to avoid an explicit treatment of solvent molecules by instead invoking a dielectric continuum. In this case solvent molecules are replaced by a uniform continuum with a suitable dielectric constant. A further, commonly used, simplification is to treat the protein as a rigid body. Sometimes simple shapes are also assumed, e.g., hard spheres (Tanford & Kirkwood 1957; Bratko et al., 1988). Other descriptions have used lattice models to better reproduce the irregular shape of proteins (Gilson et al., 1985).

As the protein will exclude solvent molecules, the question arises as to what one should choose for the dielectric permittivity of the interior region. A seemingly viable choice is the electronic permittivity (Harvey, 1989). However, this may lead to an underestimation as the assumption of a fixed protein structure precludes a dielectric response due to nuclear motions. Furthermore, it is not apparent where one should locate the dielectric boundary between the protein and solvent. A common choice is the so-called "solvent-accessable surface" (SAS) (Harvey, 1989), which is the surface traced out by a solvent molecule as it rolls over the bare protein. A model invoking a Stern layer (Stern, 1924) gives a discontinuity that is shifted outward with respect to the SAS. On the other hand, one may expect that, in reality, water is able to penetrate the

0006-2960/91/0430-5209$02.50/0

protein surface to some degree. This would then imply a shifting inward of the surface of discontinuity.

The presence of a discontinuity severely complicates the electrostatic interactions, and, in order to preserve simplicity, we have assumed *no discontinuity* in the model presented here. That is, the interior of the protein is assumed to have the same dielectric constant as the solvent! Though at first sight this may appear a rather drastic assumption, recent MC simulations (i.e., exact solutions) of a model of this type accurately reproduced observed changes in the calcium-binding affinity of bovine calbindin D_{9k} (Svensson et al., 1990). Furthermore, we show in the appendix, using a simple spherical model, that the position of the boundary has a rather strong effect on the predicted affinities. Our calculations suggest that displacing the surface a few ångströms inward of the SAS significantly lessens the effects of the discontinuity, which lends credence to the simple model used here.

Recently, the Poisson–Boltzmann (PB) and linearized PB (LPB) approximations have been numerically solved for protein models similar to that described here. The LPB theory is more popular due to its numerically more stable behavior (Sharp & Honig, 1989, and references therein). Application of these approximations to certain biomolecular systems has led some authors to emphasize the importance of the low dielectric interior of biomolecules. On the basis of our previous studies, this is apparently not the case for calbindin D_{9k} and may not be so for other ion-binding proteins as well. Clearly, more comparisons between our model and careful and varied experiments are necessary to resolve this question. Furthermore, it must be remembered that the PB and LPB are approximations and their accuracy in such applications need to be assessed.

Our previous work briefly reported experimental and theoretical shifts of the total binding constant of Ca^{2+} upon mutation of the protein and variation in the concentration of an ambient 1:1 electrolyte (KCl). For completeness, those results are also presented here, though in more detail, allowing for a more complete discussion of the mechanisms behind the shifts. The main aim of this article, however, is to report new experimental results and theoretical predictions for binding-constant shifts in calbindin, which are interesting per se but also lend further support to the simple model proposed by us. In particular we will consider the effects on the binding constant of adding a multivalent salt (K_2SO_4) to the protein solution. We also extend the theoretical analysis by looking at other types of salt valencies and expose a fundamental failure of the LPB in these cases.

Recent experiments have been successful in cleaving the calbindin molecule into two halves each containing a calcium-binding site. The electrostatic environment around the binding sites is significantly altered in the separate fragments, leading to huge shifts in the binding constant and an excellent system with which to test our model.

In addition to these direct comparisons with experiment, we also present some theoretical binding-constant shifts upon changes in the protein concentration and pH. We also discuss the possibility of competitive binding of other species and present some theoretical predictions.

Calbindin D_{9k}

General Properties. Calbindin D_{9k} is a globular protein of 75 amino acid residues and a molecular weight around 8500. It belongs to a class of structurally related intracellular regulatory Ca^{2+}-binding proteins (Rasmussen, 1986a,b). Other members of this group are troponin C, calmodulin, and parvalbumin. The binding sites of these proteins contain the same

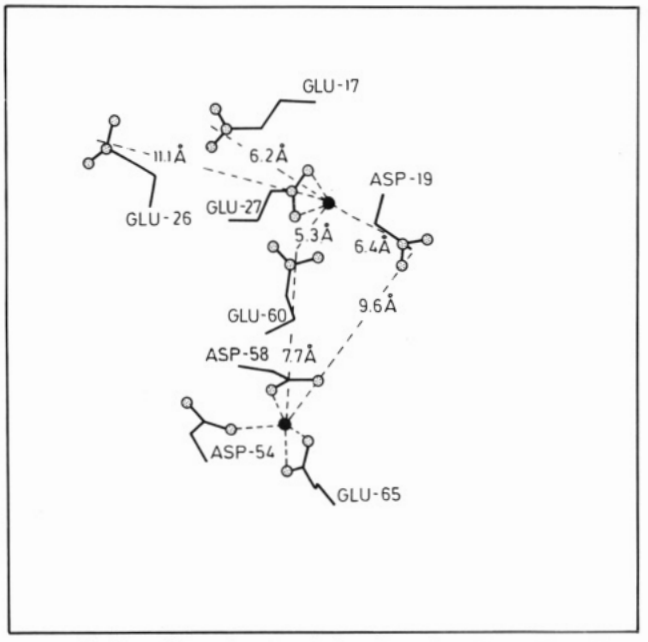

FIGURE 1: Locations of some of the charged amino acid residues relative to the Ca^{2+} sites (●) in crystalline calbindin D_{9k}. Distances are from the midpoint of the carboxylic oxygens to the Ca^{2+} ions.

helix–loop–helix arrangement, commonly referred to as an EF hand (Moews & Kretsinger, 1975). Calbindin has two binding sites that are capable of binding two Ca^{2+} ions with high affinity. Furthermore, the binding of Ca^{2+} shows significant cooperativity (Linse et al., 1987). The sites are surrounded by several negative carboxylic groups as schematically shown in Figure 1. The net charge of the apo form of the recombinant wild-type protein is -8, assuming the N-terminal methionine to be acetylated. All of the charged amino acids are close to the surface of the protein.

Experimental Studies of Calcium Binding. The macroscopic binding constants K_1 and K_2 refer to the binding of the first and second calcium ion to the protein, irrespective of which site is occupied. Thus

$$K_1 = \frac{[\mathrm{PrCa}]}{[\mathrm{Pr}][\mathrm{Ca}^{2+}]} \quad \text{and} \quad K_2 = \frac{[\mathrm{PrCa_2}]}{[\mathrm{PrCa}][\mathrm{Ca}^{2+}]} \tag{1}$$

where [Pr] and $[Ca^{2+}]$ are the concentrations of free protein and calcium, respectively, and [PrCa] and $[PrCa_2]$ are the concentrations of protein with one and two bound calciums, respectively. These binding constants were obtained from titrations of the protein (20–30 μM) with Ca^{2+} in the presence of a chromophoric Ca^{2+} chelator (30 μM of either Quin2 or 5,5′-Br_2BAPTA) at 298 K in 2 mM Tris-HCl, pH 7.5. The binding constant of the chelator was determined separately. The technique has been described in detail elsewhere (Linse et al., 1991).

The total binding constant defined as $K = K_1K_2$ and also represented as

$$pK = -\log_{10} K \tag{2}$$

was in fact determined with greater precision than either K_1 or K_2 due to the high cooperativity in binding. In this work we will confine our study to the total binding constant only.

The total binding constants of mutants of calbindin in KCl solutions of various concentrations were recently measured (Linse et al., 1988, 1991). In each mutant, one or more of the negatively charged amino acids glutamate (E) and aspartate (D) were replaced by the neutral glutamine (Q) and asparagine (N), respectively. Since the exchanged amino acids were sterically very similar and located on the surface of the

protein, this choice ensured a small perturbation of the protein structure. All possible single, double, and triple mutants involving the substitutions E17Q (Glu17 → Gln), D19N, and E26Q were investigated, as well as mutant E60Q. Here we present new experimental data and theoretical comparisons for mutants E17Q and (E17Q + D19N + E26Q) in K_2SO_4 solutions. Theoretical studies have shown that the inadequacies of the PB approximation become more obvious in the presence of multivalent ions (Wennerström & Jönsson, 1988). Furthermore, nonlinear effects in such systems may invalidate the use of the more popular LPB approximation. These considerations make the new experimental studies invaluable in assessing various theoretical approaches.

Though the mutations described above are simple and apparently minimal, they induce significant changes to the calcium-binding efficacy of calbindin. Nevertheless, more drastic changes can be made, and recently the calbindin molecule was successfully cleaved into two fragments, each containing a Ca^{2+}-binding site.[1] The cleavage was done between units 43 and 44, with the introduction of a positive and negative charge at the new ends. The N-terminal NH_2 of the first fragment had no protection group. The net charges of the fragments were −1 and −6, respectively. The two fragments were separated, and the Ca^{2+}-binding constants were measured by using NMR in water solution at neutral pH and with no added salt. The fragment concentration was 5 mM.

Theory

The Model. ^1H NMR studies indicate that the solution structure of calbindin is very similar to its crystalline form (Kördel et al., 1989). Thus the protein atoms in our fixed model were placed according to coordinates PDB31CB of the Brookhaven Protein Data Bank, which were obtained from an X-ray diffraction study of the crystalline Ca^{2+}-loaded protein (Szebenyi et al., 1981; Szebenyi & Moffat, 1986). The Brookhaven coordinate list does not include hydrogen atoms, and polar hydrogen atoms were hence added on the appropriate atoms. This was done with simple geometrical constraints, while nonpolar hydrogens present on CH, CH_2, and CH_3 groups were neglected. The total number of protein atoms included was 722. Each protein atom was represented as a hard sphere, impenetrable to any solvent ions. The number of carbon, hydrogen, oxygen, and nitrogen atoms present in the protein model were 384, 122, 91, and 125, respectively, and the hard core diameters was 3.6, 2.0, 3.2, and 3.3 Å, respectively.

A simple charge distribution on the protein atoms was used. All negatively charged carboxylic oxygens were given a charge of −0.5. These were located on glutamate and aspartate residues as well as on the C-terminal residue. The positively charged residues, which were lysines only, carried a positive unit charge on the ζ-nitrogen. All other atoms were kept neutral, including the N-terminal amino group, giving only 46 charges for the wild-type protein. Mutations were simply handled by adding a +0.5 unit charge to both oxygen atoms in the carboxylic group to turn into a neutral "amide group".

The protein was placed in the center of a spherical cell, to which counterions and salt ions were added. These were treated as mobile charged hard spheres confined in the cell. The hard core diameter of the ions, including calcium, was 4.25 Å in most of the simulations. This number has previously been used in simulations to reproduce experimental activity coefficients in simple electrolyte solutions (Card & Valleau, 1970). The cell radius was chosen so as to correspond to the actual protein concentration. The solvent was treated as a uniform dielectric continuum throughout the cell. The only way it enters the calculations is through the relative dielectric constant ϵ. The interaction energy between charged species i and j is thus given by

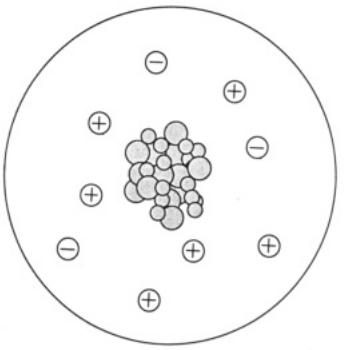

FIGURE 2: Simulated cell with ions and protein. The free ions are shown as open circles with a charge, whereas the protein atoms are filled circles.

$$u(r_{ij}) = q_i q_j e^2/4\pi\epsilon_o\epsilon r_{ij} \qquad r_{ij} \geq (\sigma_i + \sigma_j)/2 \tag{3a}$$

$$u(r_{ij}) = \infty \qquad r_{ij} < (\sigma_i + \sigma_j)/2 \tag{3b}$$

where q is the valency, e the elementary charge, ϵ_o the permittivity of free space, and r_{ij} the distance between the particles i and j. These potentials constitute the so-called primitive model for electrolyte solutions (Friedman, 1962). Only interactions with particles within the cell were taken into account. The dielectric constant and temperature were chosen to be 78.7 and 298 K, respectively, in order to correspond to water at room temperature. A schematic diagram of the system is given in Figure 2.

Monte Carlo Simulations. The simulations were performed in the canonical ensemble, where, in addition to the temperature, the number of particles and the cell volume are kept constant (Metropolis et al., 1953). At each attempted particle move, a check for hard core overlap with other particles was made. It was not necessary to always include the several hundred protein atoms in this check. Instead, the smallest possible sphere enclosing the protein atoms was calculated at the start of the simulation. After an ion move, it was checked whether the new position was closer to the center of the cell than the sum of the protein radius and the ion radius. If this was the case, hard core overlaps with the protein atoms were then checked for. Since this event was relatively rare, hard core interactions with the protein atoms consumed only a small part of the computing time (Teleman et al., 1990). At the start of a simulation, a few thousand configurations per ion were generated to allow the system to equilibrate. After this, at least 10000 configurations per ion were collected to generate the average properties. The CPU time on an IBM 3090 VF ranged from a few minutes up to about half an hour.

Binding Free Energies. We denote the so-called *microscopic* binding constants to the individual Ca^{2+} sites, labeled I and II, as K_I and K_{II}, respectively. The binding constant of site II when site I is bound is denoted as $K_{II,I}$, and vice versa. As the binding is cooperative, $K_{II,I}/K_{II} = K_{I,II}/K_I > 1$.

The following relations for the *macroscopic* binding constants K_1 and K_2 are easily derived:

$$K_1 = K_I + K_{II} \tag{4a}$$

$$K_2 = K_I K_{II,I}/(K_I + K_{II}) \tag{4b}$$

The total binding constant is thus given by

[1] J. Kördel, personal communication.

$$K = K_1K_2 = K_IK_{II,I} = K_{II}K_{I,II} \quad (4c)$$

Consider the free-energy changes upon binding Ca^{2+} ions to each of the sites. It is convenient to imagine this as a two-step process. In the first step, we envisage constraining the unbound protein so that it adopts configurations consistent with there being Ca^{2+} ions present in the binding sites. The free-energy cost associated with such a constraint will always be positive. In the second process, two Ca^{2+} ions are transferred from solution to the (preformed) sites of the constrained protein. There are many contributions to the free-energy change associated with this process. The electrostatic contribution, denoted as ΔG_{el} and which concerns us in this work, is the difference in *electrostatic* free energy of the systems corresponding to the bound and free calcium states. The rest of the free-energy contributions, ΔG_{rest}, are due to, e.g., hydration and ligand-binding energies. These latter contributions are assumed to be relatively invariant to the mutations and changes in salt concentrations considered here.

The stiff protein model used here would be unable to provide an estimate for the free energy associated with structural changes in the protein that occur in the first step of the process envisaged above. However, high-resolution ^1H NMR studies indicate that the solution structure of calbindin is very similar both in the calcium-loaded (Kördel et al., 1989; Linse et al., 1990)[2] and calcium-free (Skelton et al., 1990a,b; Linse et al., 1990) forms. Similar studies of the calcium-loaded mutants have shown that the substitutions E17Q, E26Q, and E60Q cause no significant structural changes, whereas the substitution D19N might result in small-scale rearrangements in the loop region (Linse et al., 1991). It was also shown that KCl addition causes no structural perturbation of the calcium-free wild-type protein (Linse et al., 1991). These facts suggest that free-energy contributions due to structural changes may be small or at least relatively constant over the range of mutant types and salt concentrations studied. This being the case, and assuming that ΔG_{rest} is also constant, then ΔG_{el} alone is sufficient to explain the observed shifts in K upon mutation and changes in the surrounding electrolyte. That is changes in pK with respect to a particular reference state can be obtained by using

$$pK - pK^{ref} = \beta(\Delta G_{el} - \Delta G_{el}^{ref})/\ln 10 \quad (5)$$

with $\beta = k_BT$, where T is the temperature and k_B is Boltzmanns constant.

The Modified Widom Method. Our aim is thus to calculate ΔG_{el} from simulations for a range of different mutant types and for several salt concentrations. We can write this quantity as

$$\Delta G_{el} = \mu^{ex}(2B) - 2\mu^{ex}(F) \quad (6)$$

where $\mu^{ex}(2B)$ is the excess chemical potential of the two bound calcium ions and $\mu^{ex}(F)$ is the excess chemical potential of the free ion. These excess chemical potentials were calculated with a modified Widom technique, recently developed for electrolyte solutions (Widom, 1963; Svensson & Woodward, 1988). The traditional Widom procedure is to introduce a test particle, the calcium ion, at a position $\mathbf{r}$, say one of the binding sites. If we denote as $v(\mathbf{r})$ the change in energy of the system, the excess chemical potential of the test particle at $\mathbf{r}$ is then obtained as

$$\beta\mu^{ex}(\mathbf{r}) = -\ln \langle \exp[-\beta v(\mathbf{r})] \rangle \quad (7)$$

The angular brackets denote an ensemble average over the salt particles, which behave as if they do not see the test particle. Equation 7 is valid for an infinitely large system. However, a finite system, such as our simulation box or cell, does not allow for nonelectroneutral fluctuations that can favorably interact with an inserted test charge and hence give a significant contribution to the average. Given the long range of the coulombic interactions, a large error can ensue from a straightforward application of eq 7. A simple charge-scaling procedure (Svensson & Woodward, 1988) can correct for much of this error. This approach has been successfully applied to both uniform and nonuniform electrolytes.

With the modified Widom method, the excess chemical potential of the bound ions, $\mu^{ex}(2B)$, was obtained by introducing the test particles at the binding sites, as specified in the crystal structure. In the presence of salt, an accurate estimate of $\mu^{ex}(2B)$ could be obtained with a much smaller cell size than specified by the actual protein concentration. This is due to the efficient screening of the protein charge and led to much reduced computation times. However, the same procedure would lead to errors in our estimates for $\mu^{ex}(F)$. This is because, for dilute protein concentrations and for the salt concentrations considered here, a *free* calcium ion would see mainly a uniform salt solution. A better estimate was then obtained by simulating the isotropic salt solution at the appropriate concentration. When no additional salt is present, however, or when the protein concentration becomes comparable with that of the salt, the chemical potential of the free calcium is more consistently evaluated by randomly placing the test particle in the cell containing the protein and the appropriate amount of salt and counterions.

Results and Discussion

Effects of Mutation and KCl. A series of simulations of 20 μM mutant calbindin were performed in various KCl solutions corresponding to the experimental systems (Linse et al., 1988, 1991). In a previous article we reported the total shifts in pK calculated from these simulations (Svensson et al., 1990). In order to obtain a more complete understanding of the mechanisms behind the shifts, we present here the separate chemical potential contributions appearing in eq 6; these are given in Table I. The *static* contribution, due only to the sum of the bare protein charges (no counterions and no added salt), is listed separately for each mutant.

For a salt-free counterion-only system, the excess chemical potential of free calcium varies with the type of mutant. This is so because the electric field from the protein is only weakly screened by the counterions; the screening length in the salt-free systems varies between 300 and 400 Å. When the salt concentration reaches 0.05 M, the free calcium ion essentially does not sense the protein at all, and we use the chemical potential as determined from a uniform KCl solution at the same concentration. An interesting feature is that addition of very small amounts of KCl to a salt-free protein solution initially increases the excess chemical potential of free Ca^{2+}. Upon further addition of salt, it will start to decrease and eventually become more negative than the initial value.

The theoretical and experimental numbers that should be compared are the *shifts* in the total binding constants or, more precisely, $\Delta pK = pK - pK^{ref}$. These are also listed in Table I. The wild-type protein in salt-free solution has been chosen as the reference. As the protein has a larger absolute charge than calcium ions, most of the shift in pK comes from the chemical potential of the bound ions. These depend strongly on the salt concentration and are largest for the wild-type protein, which is the most charged mutant. This may not be the case for proteins or mutants with smaller charges, whereby

[2] J. Kördel and W. J. Chazin, personal communication.

Table I: Excess Chemical Potential of Free and Bound Ca^{2+} and Simulated and Experimental Shifts in the Total Binding Constant for Mutants at Various Concentration of KCl[a]

protein	C_{KCl} (M)	$-\beta\mu^{ex}$ (Ca^{2+},F)	$-\beta\mu^{ex}$ (Ca^{2+},2B)	ΔpK	ΔpK^{exp}
wild-type			36.56		
	0.00	0.84	35.49	0.00	0.0
	0.05	0.85	29.36	2.67	2.9
	0.10	1.07	28.27	3.34	3.6
	0.15	1.21	27.77	3.67	4.0
E17Q			33.26	1.43	
	0.00	0.42	32.38	0.99	1.2
	0.05	0.85	27.44	3.50	3.4
	0.10	1.07	26.46	4.12	4.0
	0.15	1.21	25.92	4.48	4.2
(E17Q + D19N)			29.54	3.05	
	0.00	0.28	28.86	2.39	2.4
	0.05	0.85	25.14	4.50	4.1
	0.10	1.07	24.32	5.05	4.6
	0.15	1.21	23.95	5.33	4.9
(E17Q + D19N + E26Q)			27.43	3.97	
	0.00	0.23	26.93	3.19	3.4
	0.05	0.85	24.14	4.94	4.8
	0.10	1.07	23.48	5.42	5.3
	0.15	1.21	23.16	5.68	5.4

[a] The first line for each mutant gives the static contribution. The estimated errors in the chemical potentials for free and bound are less than 0.02 and 0.1, respectively. The estimated errors in the simulated and experimental shifts in pK are less than 0.05 and around 0.1, respectively.

the chemical potentials of the free ions may be important. The excellent agreement between theory and experiment supports our simple model. This is true even for shifts in pK of up to five units (five orders of magnitude in K!). It is only for one mutant, E60Q, that simulations deviate from experiments. This may be due to a difference in the position of the charged group of residue 60 in the solution as opposed to the crystalline form. A recent molecular dynamics simulation showed that this may be the case (Ahlström et al., 1989). Another possibility is that the position of the charged group is markedly different in the apo and the Ca^{2+}-loaded proteins.

The simulated shifts in the binding constant are insensitive to the details of the model. For example, a more detailed charge model that used partial charges on all protein atoms, taken from the molecular dynamics program package MUMOD (Ahlström et al., 1989), has also been tried. The difference between the two models is much smaller than the shifts observed (Svensson et al., 1990). Obviously, the long-range character of the coulombic interactions makes the difference between the two charge models insignificant. Neither does the shift depend dramatically on the hard core diameters, as long as they are within reasonable limits. Changing the Ca^{2+} diameter from 4.25 to 2 Å for the wild-type protein in 0.15 M KCl increases ΔpK by 0.2 unit. For the same system, discarding all the hydrogen atoms of the protein increases ΔpK by only 0.1 unit.

The agreement with experimental data could be further improved by adding salt at a concentration of a few millimolar to the salt-free system, in order to account for the buffer and chelator present in the experiment. Furthermore, there might also be a small residual ionic concentration in the purified protein solution. However, considering the agreement already obtained in Table I and the experimental uncertainties, it seems pointless to manipulate the parameters in order to improve the agreement.

Effect of Multivalent Electrolytes. In order to test the effects of a multivalent salt on calcium binding, experiments

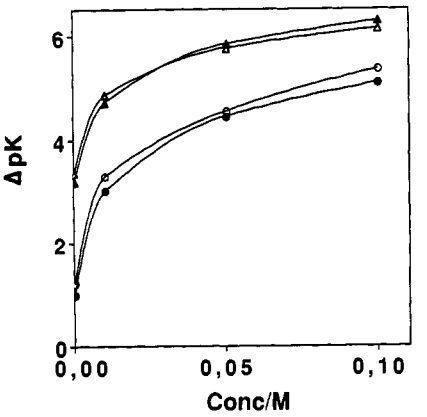

FIGURE 3: Experimental versus simulated ΔpK for E17Q and (E17Q + D19N + E26Q) in various K_2SO_4 solutions: E17Q, simulation (●) and experiments (○); (E17Q + D19N + E26Q), simulation (▲) and experiments (△). The wild-type protein in salt-free solution has been chosen as a reference.

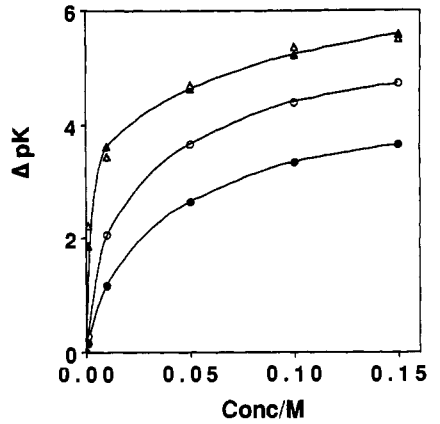

FIGURE 4: Simulated shifts for 20 μM wild-type protein in various electrolyte solutions: 1:−1 (●), 1:−2 (○), 2:−1 (▲), and 2:−2 (△) electrolytes. The salt-free solution has been chosen as a reference.

were carried out on the wild-type protein and the mutants E17Q and (E17Q + D19N + E26Q) in 0.01, 0.05, and 0.10 M K_2SO_4. A divalent anion (rather than cation) was chosen in order to avoid the possibility of competitive binding. Figure 3 compares these experiments with simulations where the wild-type protein in salt-free solution has again been chosen as a reference. Once again our model shows remarkable agreement with experiment, even for shifts up to six orders of magnitude!

Simple screening arguments would lead us to expect that K_2SO_4 would induce larger shifts than KCl. For example, in the LPB approximation, the ambient electrolyte enters the theory via the inverse Debye screening lengh κ with

$$\kappa^2 \propto \sum_i \rho_i q_i^2 \qquad (8)$$

where ρ_i is the density of the ith type of ion in solution. At the same molarity, κ^2 is three times larger for the K_2SO_4 solution, giving rise to larger screening effects and hence bigger shifts. Figure 4 shows the simulated shifts in pK of the wild-type protein as a function of salt concentration for these electrolyte solutions and confirms our conjecture.

It is straightforward to extend the theoretical calculations to include divalent cations. Competitive binding will of course not be a problem in our theoretical experiments, and all effects will be due to electrostatics. Thus we also studied hypothetical 2:−1 and 2:−2 electrolytes. If one was to believe the LPB approximation, the effects of a 2:−1 and a 1:−2 electrolyte would be indistinguishable as they would have identical Debye

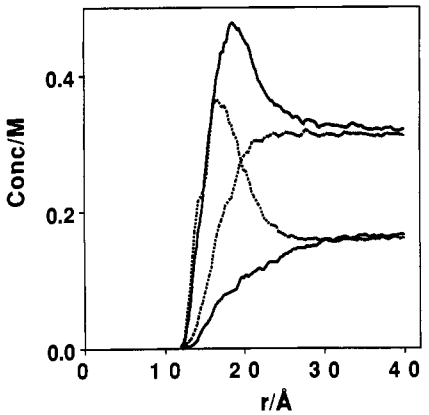

FIGURE 5: Radial concentration of co- and counterions in the cell. The results are for 20 μM wild-type protein in 0.15 M 1:−2 (—) and 2:−1 (···) electrolytes.

Table II; The Shifts in the Individual Microscopic Binding Constants ΔpK_i of the Two Fragments of Wild-Type Calbindin[a]

fragment	ΔpK^0_i	ΔpK_i	ΔpK	ΔpK^{exp}
1	3.79 (3.67)	3.42 (3.42)		
			4.94 (5.04)	5.7
2	1.16 (1.16)	2.54 (2.64)		

[a] The shifts are calculated relative to the corresponding sites in 20 μM wild-type calbinding in a salt-free solution. The concentration of the fragments is 5 mM, and no salt has been added to the solutions. The second column shows the static part of the change, while the last two columns show the simulated and experimental shifts in the total binding constant. Results for the detailed charge model are within parentheses. The errors in the simulated and experimental numbers are estimated to be less than 0.05 and 0.3, respectively.

screening lengths. Figure 4 shows this not to be the case; instead we see that the 2:−1 and 2:−2 electrolytes give very nearly the same shifts, which are much larger than the 1:−2 case. This fits in with the intuitive idea that since calbindin has a large negative net charge, it is the nature of the cation that determines the effect on the binding constant. For example, at concentrations around 10^{-3} M, the solutions containing the monovalent cation both show small effects. This is not the case for divalent cations, where even such small concentrations cause a decrease in the Ca^{2+} affinity of about 2 pK units.

It is feasible that one can circumvent the problem of competitive binding by using a sufficiently bulky divalent cation that would be too large to bind. We thus tested the effect of ionic size on the pK shifts. At 0.15 M salt solution, a change of the diameter of the divalent ion from 4.25 to 8 Å decreases ΔpK by 0.2 and 1.0 unit for the 1:−2 and 2:−1 salt, respectively. At lower salt concentration, the effect will be smaller in both cases.

Figure 5 shows the concentration of ions as a function of distance from the center of the cell for the wild-type protein in 0.15 M 1:−2 and 2:−1 salt. The large negative net charge of the protein causes an accumulation of cations near the protein.

Calbindin Fragments. When considering the cleaved protein, it was assumed that the structures of the individual fragments were identical with the intact calbindin molecule, and all atoms not present in a particular fragment were discarded. In the experiments, the fragments were separated, and the individual binding constants K_I and K_{II} were measured. A "total" binding constant defined by the product K_IK_{II} could then be compared with K_1K_2 of the intact protein. Table II shows the comparison between the experimental and theoretical shifts in pK for the cleaved wild-type protein in a salt-free solution. The results of the detailed charge model for the protein with MUMOD fractional charges are also shown. Given the fact that the shift is enormous, the agreement between theory and experiment is impressive.

Table III: Shifts in the Binding Constant for M^+ and Ca^{2+}, without (ΔpK) and with (ΔpK^c) the Assumption of Strong Binding of M^+ [a]

protein	C_{KCl} (M)	ΔpK (M^+)	ΔpK (Ca^{2+})	ΔpK^c (Ca^{2+})	ΔpK^{exp}
wild-type	0.00	0.00	0.00	0.00	0.0
	0.01	1.00	1.17	0.17	
	0.05	1.68	2.67	0.99	2.9
	0.10	1.99	3.34	1.35	3.6
	0.15	2.17	3.67	1.50	4.0
(E17Q +		1.98	3.97	1.99	
D19N +	0.00	1.82	3.19	1.37	3.4
E26Q)	0.01	2.34	4.05	1.71	
	0.05	2.81	4.94	2.13	4.8
	0.10	3.02	5.42	2.40	5.3
	0.15	3.14	5.68	2.54	5.4

[a] The reference was choosen as 20 μM wild-type protein in salt-free solution and with M^+ as counterions. The first line for each mutant gives the static shifts.

Competitive Binding of Monovalent Ions. Table I shows that the electrostatic potential is strongly negative in the binding sites. Thus, one might also anticipate that monovalent cations, M^+, can bind to the same sites. As for Ca^{2+}, addition of KCl decreases the binding constant of M^+. The result for the wild-type protein and (E17Q + D19N + E26Q) is shown in Table III. Compared to binding of Ca^{2+}, there is a weaker salt dependence. Having both Ca^{2+} and M^+ present in a solution may create a competition for the binding sites. A detailed analysis of how this competition depends on the mutant ion and the added salt requires a knowledge of the microscopic binding constants for both types of ions. Unfortunately, these constants are difficult to measure experimentally. However, a simple limiting case is when all protein molecules bind two M^+ in its Ca^{2+}-free state. This would be the case for a concentration of M^+ that is large compared to its dissociation constant. Binding of Ca^{2+} could then be considered as

$$Pr(M^+)_2 + 2Ca^{2+} \rightarrow Pr(Ca^{2+})_2 + 2M^+ \quad (9)$$

The simulated Ca^{2+} shifts corrected for competitive binding will then become

$$\Delta pK^c\ (Ca^{2+}) = \Delta pK\ (Ca^{2+}) - \Delta pK\ (M^+) \quad (10)$$

From the results in Table III and the comparison with experimental results, we conclude that K^+ is not likely to bind competitively. This can be a result of the lower charge and/or the larger ionic diameter of K^+, which may exclude it from the sites. NMR spectroscopic investigations seem to support this conclusion (Linse et al., 1991).

Variation of Protein Concentration. The experimental studies were made with a protein concentration around 20–30 μM. Since the counterion concentration increases with protein concentration, it is reasonable to expect that this will affect the binding constants. A set of simulations were made at protein concentrations ranging from 10^{-7} to 10^{-2} M. In Figure 6, the shifts in pK relative to infinite dilution of the wild-type protein and (E17Q + D19N + E26Q) are shown as a function of protein concentration with and without 0.15 M KCl. In the absence of salt, the counterions themselves will screen the electrostatic interactions and with increasing protein concentration cause a gradually larger positive shift in pK. We can also rationalize the results in the following terms: a high

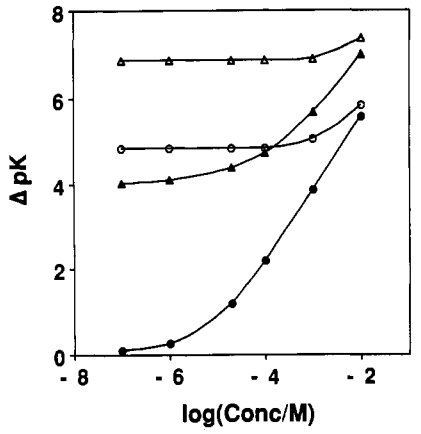

FIGURE 6: Simulated shifts for wild-type protein and (E17Q + D19N + E26Q) at various concentrations of protein, without salt and with 0.15 M KCl: wild-type, no salt (●) and 0.15 M KCl (○); (E17Q + D19N + E26Q), no salt (▲) and 0.15 M KCl (△). The wild-type protein at infinite dilution in salt-free solution is chosen as a reference.

protein concentration gives a small cell size, which decreases the free energy of a free Ca^{2+} ion, while at the same time an increased counterion concentration leads to more effective screening of the interaction between the protein and the bound Ca^{2+}, raising the free energy of the latter.

Increasing an initially very dilute protein concentration in a solution of 0.15 M KCl hardly has any effect. This is so because the salt will completely dominate the screening at submillimolar protein concentrations, and it is only when the protein concentration exceeds about 1 mM that the counterions start to contribute to the screening. This is clearly demonstrated in Figure 6 as a small difference between the systems with and without salt at the largest protein concentrations.

pH Dependence. A change in pH would cause a protonation or deprotonation of some residues in the protein, which indirectly would affect the binding constant. If the pK values of the individual residues in the protein were known, it would be a straightforward task to calculate shifts in the binding constants, using the present model. Since this information is not available, we have chosen to calculate the expected shifts in the binding constant upon making the solution sufficiently acidic or basic. The acidic solution (low pH) corresponds to the situation where all of the 18 carboxylic groups on the glutamic and aspartic residues are protonated. The basic solution (high pH) is that where all 10 lysine residues are neutralized. Thus for these cases the apo protein would have a net charge of +10 and −18, respectively. With such a large number of charged groups changed, we expect dramatic changes in the binding constants.

Let us consider an infinitely dilute protein solution. At low pH, the model predicts all mutants in the study to have the same binding constant, since a mutation under these circumstances will not change the charge of the protein, *nota bene* the only mutations we have studied are neutralization of acidic groups. Since the protein is highly charged at both low and high pH, we anticipate that the addition of salt or increasing the protein concentration induces large shifts in the binding constant. In performing these simulations, we have assumed that both the apo and the Ca^{2+}-loaded protein is stable with respect to changes in pH. This is true for moderate changes (Wendt et al., 1988) but probably not in the extreme limits chosen here. Nevertheless, one can use these calculations as lower and upper bounds for absolute shifts in pK upon these large pH changes. Table IV shows the resulting pK shifts for the wild-type protein in 0.15 M KCl. The reference here is the wild-type protein at neutral pH, with the same salt concentration. Also shown are the purely static shifts, due to changes in the bare protein charges. These are calculated relative to the wild-type protein at neutral pH. The observed shifts are large as is their salt dependence. An interesting situation to test experimentally is the calcium binding at high pH, where one may expect an increased binding by several orders of magnitude compared to that at neutral pH.

Table IV: Shifts in Binding Constant of Wild-Type Protein at Low and High Solutions pH[a]

pH	ΔpK^0	ΔpK
low	24.58	14.09
high	−7.59	−1.97

[a] Results are shown for infinitely dilute wild-type protein in 0.15 M KCl solution. The static part of the change (ΔpK^0) is also shown. As a reference we use the wild-type protein in neutral solution at the same salt concentration. The estimated error is less than 0.1.

CONCLUSIONS

The convincing agreement between theory and the experimental data presented here shows that our simple dielectric continuum model for calbindin has a firm physical basis. As is shown in the appendix, the introduction of a low dielectric region for the protein interior would significantly worsen the agreement between experiment and theory. The results with multivalent salts show that the theory still remains accurate under more extreme electrostatic conditions. We predict that addition of 1:2 salt has a very different screening effect, depending on the sign of the divalent ion, which is contrary to the linear theory with its dependence on the single parameter κ. If the divalent ion has a charge of opposite sign to the protein, then even as low a salt concentration as 10^{-3} M will screen the binding sites significantly. The full PB treatment will be necessary under such conditions but may prove to be difficult to solve in the presence of divalent salt species.

Correlations between the binding sites and the ensuing cooperativity make the interesting system of the cleaved protein more difficult to treat. Nevertheless, our theoretical results suggest that most of the shift in pK measured for this system comes from the electrostatic contribution.

In addition to the direct comparisons with experiment, we have also investigated other systems using the theoretical model. These include a study of competitive binding by monovalent cations and the effects of varying the protein concentration and pH.

A basic assumption in the present approach, which seems to be fulfilled, is that the Ca^{2+}-bound protein structures are not significantly different when the protein is placed in salt solutions, at least for the concentrations considered here, even for mutations of the charged amino acids. The more difficult question of why it is possible to assume a high dielectric constant for the interior (the same as for water) of the protein is as yet unanswered, but together with the new experimental results presented here the evidence is most convincing. One possible reason is that water is able to significantly penetrate the protein surface, putting any dielectric boundary a few ångströms inside the usual solvent-accessible surface.

Finally we want to point out the simplicity and efficiency of the Monte Carlo technique applied here. We feel that it has great potential for studies of electrostatic effects in complex biochemical systems.

APPENDIX

In a uniform dielectric medium, Coulombs law takes the same form as in a vacuum, but scaled by the relative dielectric permittivity of the medium. In a medium that contains a

Table V: Additional Contribution from a Low-Permittivity Interior of the Protein to the Static Shift[a]

mutant	exp	no disc	10 Å	12 Å	13 Å	14 Å	15 Å
E17Q	1.21	1.43	0.22	0.21	0.24	2.81	5.25
D19N	1.31	1.61	0.31	0.33	0.33	1.01	4.18
E26Q	0.51	0.92	−0.02	−0.04	−0.04	−0.42	1.18
E60Q	0.32	1.98	0.42	0.40	3.82	7.76	11.24

[a] See eqs A1–A3. The results are shown as a function of the radius of the sphere enclosing the medium with low permittivity. The experimental result at the lowest ionic strength and the calculated result with no discontinuity are shown in the second and third columns.

dielectric discontinuity, the presence of a charge will cause polarizations at the interface, which complicates this simple expression (Jackson, 1975). The polarization can be handled in different ways. It can of course be incorporated into a numerical solution of Poissons equation by, for example, a grid technique (Warwicker & Watson, 1982). For some particularly simple geometries, the polarization can also be formulated in terms of image charges, that is, a real charge in one medium will create an image charge in the other medium (Friedman, 1975; Barrera et al., 1978).

For a sphere of low permittivity ϵ_1 with a radius a immersed in a high-permittivity solvent ϵ_2, the image approach becomes tractable. Consider the potential $\phi(\mathbf{r})$ of a charge q at position $\mathbf{r}_1$, where we have taken the origin to be at the center of the low-permittivity sphere. Depending on the positions of $\mathbf{r}$ and $\mathbf{r}_1$ with respect to the dielectric discontinuity, we have different expressions:

$$\phi(\mathbf{r}) = \sum_{l=1}^{\infty} \frac{l}{1+l} \frac{\epsilon_2 - \epsilon_1}{\epsilon_2 + \epsilon_1 l/(l+1)} \frac{a^{2l+1}}{r_1^{l+1}} \frac{q}{\epsilon_2 r^{l+1}} P_l(\cos\gamma) + \frac{q}{\epsilon_2|\mathbf{r} - \mathbf{r}_1|} \qquad r, r_1 > a \quad \text{(A1)}$$

$$\phi(\mathbf{r}) = \sum_{l=1}^{\infty} \frac{l}{1+l} \frac{\epsilon_2 - \epsilon_1}{\epsilon_2 + \epsilon_1 l/(l+1)} \frac{r^l}{r_1^{l+1}} \frac{q}{\epsilon_2} P_l(\cos\gamma) + \frac{q}{\epsilon_2|\mathbf{r} - \mathbf{r}_1|} \qquad r < a < r_1 \quad \text{(A2)}$$

$$\phi(\mathbf{r}) = -\sum_{l=0}^{\infty} \frac{\epsilon_2 - \epsilon_1}{\epsilon_2 + \epsilon_1 l/(l+1)} \frac{r_1^{l+1}}{a^{2l+1}} \frac{q r^l}{\epsilon_1} P_l(\cos\gamma) + \frac{q}{\epsilon_1|\mathbf{r} - \mathbf{r}_1|} \qquad r, r_1 < a \quad \text{(A3)}$$

where P_l is a Legendre polynomial and γ is the angle between the position vectors. However, it is still too complex to incorporate into an MC simulation unless the series is truncated at any early stage (Linse, 1986). Let us therefore restrict ourselves to the image effect on the static contribution to the binding constant shifts, i.e., in the absence of any salt or counterions. The protein model remains the same as above with the exception that we now insert a low dielectric sphere ($\epsilon_1 = 4$) whose center coincides with the center of mass of the protein. The two calcium-binding sites are situated 10.3 and 11.1 Å from the center, respectively, and the mutated amino acid residues Glu17, Asp19, Glu26, and Glu60 are found 13.0, 13.8, 13.3, and 12.0 Å from the center, respectively. Given the coordinates of the calcium sites and of the mutated residues, it is straightforward to calculate the extra contribution to the potential from the dielectric discontinuity with eqs A1–A3.

Table V shows how the magnitude of the correction due to the discontinuity varies for different mutants and with the size of the low dielectric sphere. The changes are in general rather small when the low dielectric sphere does not include the mutated charge. However, once this extends beyond the mutated charge, its effect increases rapidly, which deteriorates the excellent agreement with experiment. In the past when a low permittivity of the protein was used, it has generally extended out to the SAS of the protein. The SAS includes the protein atoms, which have a radius of 1–2 Å (Gilson & Honig, 1987). For mutant E17Q, for example, the present calculations show that this would give an additional contribution to the static shift of 3–5 orders of magnitudes.

The presence of a medium with low permittivity will of course affect the salt distribution outside the protein and thereby also the screening of the calcium sites. It is not a simple matter to predict in which direction this image effect will act. Salt ions will tend to avoid the immediate neighborhood of the low dielectric medium, but the discontinuity will also increase the coupling between the salt particles and affect the screening. The first effect can be understood as a simple one-particle correlation, while the latter has a more complex many-particle origin.

Models with a dielectric discontinuity have in the past been treated by the PB approximation (Sharp & Honig, 1989, and references therein). It is worth noting that the PB equation is an approximation that does not include, for example, electrostatic ion–ion correlations or hard core effects of the mobile ions. These mean-field approximations also have consequences on the effects due to a dielectric boundary. This can most easily be seen by considering a charged plane dividing space into two halves, one with low and the other, containing the mobile ions, with high permittivity. This system exhibits image effects in an *exact* treatment (Wennerström & Jönsson, 1988), which can give rise to strong depletions in the ion profiles close to the interface. No such effects occurs in a PB approximation, which ignores the self-image of ions. A similar situation arises in spherical geometry (Linse, 1986). In fact, the effects of a dielectric discontinuity seen in PB solutions by biomolecular models are due only to asymmetries in the mean charge distribution. As illustrated by the planar case, one totally neglects a significant contribution arising from the self-images of ions that are modulated somewhat by ion correlations. This seems not to have been appreciated by previous applications in this area.

Acknowledgments

We thank J. Kördel for giving us access to unpublished binding constants of the calbindin fragments.

Registry No. Ca, 7440-70-2; Glu, 56-86-0; Asp, 56-84-8; KCl, 7447-40-7; K_2SO_4, 7778-80-5.

References

Ahlström, P., Teleman, O., & Jönsson, B. (1987) *J. Am. Chem. Soc. 109*, 1541–1551.

Ahlström, P., Teleman, O., Kördel, J., Forsén, S., & Jönsson, B. (1989) *Biochemistry 28*, 3205–3211.

Barrera, R. G., Guzman, O., & Balaguer, B. (1978) *Am. J. Phys. 46*, 1172–1179.

Bratko, D., Luzar, A., & Chen, S. H. (1988) *Bioelectrochem. Bioenerg. 20*, 291–296.

Card, D. N., & Valleau, J. P. (1970) *J. Chem. Phys. 52*, 6232–6240.

Friedman, H. L. (1962) in *Ionic Solution Theory*, Interscience Publishers, New York.

Friedman, H. L. (1975) *Mol. Phys. 29*, 5133–5143.

Gilson, M. K., & Honig, B. H. (1987) *Nature 330*, 84–86.

Gilson, M. K., Rashin, A., Fine, R., & Honig, B. (1985) *J. Mol. Biol. 183*, 503–516.

Hansen, J. P., & McDonald, I. R. (1976) *Theory of Simple Liquids*, Academic Press, London.
Harvey, S. C. (1989) *Proteins 5*, 78–92.
Jackson, J. D. (1975) *Classical Electrodynamics*, Wiley, New York.
Klapper, I., Hagstrom, R., Fine, R., Sharp, K., & Honig, B. (1986) *Proteins 1*, 47–59.
Kördel, J., Forsén, S., & Chazin, W. J. (1989) *Biochemistry 28*, 7065–7074.
Linse, P. (1986) *J. Phys. Chem. 90*, 6821–6828.
Linse, S., Brodin, P., Drakenberg, T., Thulin, E., Sellers, P., Elmdén, K., Grundström, T., & Forsén, S. (1987) *Biochemistry 26*, 6723–6735.
Linse, S., Brodin, P., Johansson, C., Thulin, E., Grundström, T., & Forsén, S. (1988) *Nature 335*, 651–652.
Linse, S., Johansson, C., Brodin, P., Grundström, T., Drakenberg, T., & Forsén, S. (1991) *Biochemistry 30*, 154–162.
Linse, S., Teleman, O., & Drakenberg, T. (1990) *Biochemistry 29*, 5925–5934.
Metropolis, N., Rosenbluth, A. W., Rosenbluth, M. N., Teller, A. H., & Teller, E. (1953) *J. Chem. Phys. 21*, 1087–1092.
Moews, P. C., & Kretsinger, R. H. (1975) *J. Mol. Biol. 91*, 201–228.
Rasmussen, H. (1986a) *N. Engl. J. Med. 314*, 1094–1101.
Rasmussen, H. (1986b) *N. Engl. J. Med. 314*, 1164–1170.
Sharp, K., & Honig, B. (1989) *Chem. Scr. 29A*, 71–74.
Skelton, N. J., Forsén, S., & Chazin, W. J. (1990a) *Biochemistry 29*, 5752–5761.
Skelton, N. J., Kördel, J., Forsén, S., & Chazin, W. J. (1990b) *J. Mol. Biol. 213*, 593–598.
Stern, O. (1924) *Z. Elektrochem. Angew. Phys. Chem. 30*, 508–516.
Svensson, B., & Woodward, C. (1988) *Mol. Phys. 64*, 247–259.
Svensson, B., Jönsson, B., & Woodward, C. E. (1990) *Biophys. Chem.* (in press).
Szebenyi, D. M. E., & Moffat, K. (1986) *J. Biol. Chem. 261*, 8761–8777.
Szebenyi, D. M. E., Obendorf, S. K., & Moffat, K. (1981) *Nature 294*, 327–332.
Tanford, C., & Kirkwood, J. G. (1957) *J. Am. Chem. Soc. 79*, 5333–5339.
Teleman, O., Svensson, B., & Jönsson, B. (1990) *Comput. Phys. Commun.* (in press).
Warwicker, J., & Watson, H. C. (1982) *J. Mol. Biol. 157*, 671–679.
Wendt, B., Hofmann, T., Martin, S. R., Bayley, P., Brodin, P., Grundström, T., Thulin, E., Linse, S., & Forsén, S. (1988) *Eur. J. Biochem. 175*, 439–445.
Wennerström, H., & Jönsson, B. (1988) *J. Phys. (Paris) 49*, 1033–1041.
Widom, B. (1963) *J. Chem. Phys. 39*, 2808–2812.

γ-Chymotrypsin Is a Complex of α-Chymotrypsin with Its Own Autolysis Products[†,‡]

M. Harel,[§] C.-T. Su,[∥] F. Frolow,[⊥] I. Silman,[*,∥] and J. L. Sussman[*,§]
Departments of Structural Chemistry, Neurobiology, and Chemical Services, Weizmann Institute of Science, Rehovot 76100, Israel

Received June 19, 1990; Revised Manuscript Received December 11, 1990

ABSTRACT: The determination of three separate γ-chymotrypsin structures at different temperatures and resolutions confirmed the presence of electron density in the active site, which could be interpreted as an oligopeptide as had previously been suggested by Dixon and Matthews [(1989) *Biochemistry 28*, 7033–7038]. HPLC analyses of the enzyme before and after crystallization demonstrated the presence of a wide variety of oligopeptides in the redissolved crystal, most with COOH-terminal aromatic residues, as expected of the products of chymotrypsin cleavage, which appeared to arise from extensive autolysis of the enzyme under the crystallization conditions. The refined structures agree well with the conformation of both γ-chymotrypsin and α-chymotrypsin. The electron density in the active site is thus interpreted as arising from a repertoire of autolysed oligopeptides produced concomitantly with crystallization. The COOH-terminal carbons of the polypeptide(s) display short contact distances (1.97, 2.47, and 2.13 Å, respectively) to Ser195 O^{γ} in all three refined structures, but the electron density is not continuous between these two atoms in any of them. This suggests that some sequences are covalently bound as enzyme intermediates while others are noncovalently bound as enzyme–product complexes.

The serine protease γ-chymotrypsin (γ-Cht)[1] was identified as a crystalline form distinct from α-chymotrypsin (α-Cht) by Kunitz (1938) although it has a very similar conformation (Matthews et al., 1967; Cohen et al., 1981). Although α-Cht and γ-Cht are believed to be identical in primary sequence (Desnuelle, 1960), the question of whether the two crystalline forms originate from two distinct conformational species in solution has remained a matter for discussion (Corey et al., 1965; Dixon & Matthews, 1989). γ-Cht is crystallized at higher pH (e.g., 5.6 vs 4.2) than α-Cht and packs as a mo-

[†] This work was supported by U.S. Army Medical Research and Development Command Contracts DAMD17-GC-7037 and DAMD17-89-C-9063, by the Minerva Foundation, Munich, Germany, and by the U.S.–Israel Binational Science Foundation.
[‡] Coordinates (code name 8GCH) for γ-chymotrypsin (Nat-1) were deposited in the Protein Data Bank, Brookhaven National Laboratory (Bernstein et al., 1977).
* Correspondence should be addressed to these authors.
[§] Department of Structural Chemistry.
[∥] Department of Neurobiology.
[⊥] Department of Chemical Services.

[1] Abbreviations: α-Cht, α-chymotrypsin; Cht, chymotrypsin; Chtph7, γ-Cht at pH 7.0; γ-Cht, γ-chymotrypsin; OMTKY3, turkey ovomucoid inhibitor third domain; TFA, trifluoroacetic acid.

0006-2960/91/0430-5217$02.50/0